Experimental measurement of value and associated uncertainty of wave speed in Hopkinson bars with an accurate and robust method

Denis Brizard

BRIZARD, Denis, 2018, Experimental measurement of value and associated uncertainty of wave speed in Hopkinson bars with an accurate and robust method, International Conference on Uncertainty in Structural Dynamics USD, LEUVEN, BELGIQUE, 2018-09-17, 10 p

Experimental measurement of value and associated uncertainty of wave speed in Hopkinson bars with an accurate and robust method

D. Brizard [1]
[1] Univ Lyon, Universit Claude Bernard Lyon 1, IFSTTAR, LBMC UMR_T9406, F69622, Lyon, France
e-mail: **denis.brizard@ifsttar.fr**

Abstract

Post processing the strain waves in the measurement bars of Split Hopkinson Bars (SHPB) to get the stress-strain in the sample requires the knowledge of the longitudinal wave velocity c_0. In the context of metrology, we need to assess the measurement uncertainty in the value of c_0. The most intuitive way of getting the velocity c_0 relies on the measurement of the length of the bar and of the time shift between multiple reflections of a stress pulse in the bar. This method however faces some difficulties which increase the uncertainty in c_0. In this paper, we rather use a method based on the frequency spectrum of an impact test on a single bar and on the expression of longitudinal resonance frequencies. The relative uncertainty on the obtained velocity c_0 is also assessed and is lower than $0.04\,\%$: it is mainly related to the uncertainty in the length of the bar. A precise value of the velocity c_0 and of the associated measurement uncertainty is an important step in the context of SHPB to precisely assess the final uncertainty in SHPB test results, which is scarcely ever done.

1 Introduction

Split Hopkinson pressure bars is an experimental device for measuring the stress-strain relationship of materials in the intermediate range of strain rate ($100\,\mathrm{s}^{-1}$ to $10\,000\,\mathrm{s}^{-1}$) [1]. The device is composed of a striker and two measuring bars [2]. The sample lies between the two measuring bars and the striker hits the first measuring bar at a given velocity. A strain pulse propagates down the first measuring bar: part of the pulse is reflected at the interface with the sample and part of the pulse crosses the sample and propagates through the second measuring bar. The strain history in each bar is recorded with a strain gauge, this strain gauge is commonly placed in the middle of the bar to avoid overlay between the incident and reflected pulses. The stress and strain in the sample are computed from the incident, reflected and transmitted pulses in the bars.

The value of c_0 is important in the posttreatment of the SHPB tests because it is used to get the strain rate and the strain in the sample with the following equations [3]

$$\dot{\epsilon}_s(t) = \frac{-2c_0}{l_s}\epsilon_r(t) \tag{1}$$

$$\epsilon_s(t) = \frac{-2c_0}{l_s}\int_0^t \epsilon_r(\tau)d\tau \tag{2}$$

where l_s is the initial length of the sample and $\epsilon_r(t)$ is the reflected pulse measured in the input measuring bar.

In the context of quality in measurement, it is also necessary to determine the uncertainty in c_0 as it is involved in the final uncertainty in the stress and strain in the sample.

Of course it is possible to deduce c_0 from the measurement of E on a tensile testing machine and of the measurement of ρ. However, getting the value of c_0 directly from a test made on the SHPB device is appealing, especially if one does not have easily access to other facilities.

Because a SHPB device is designed to perform impact tests, an intuitive method to get c_0 would consist in the following steps: measure the length of the bar; perform an impact test on a single bar; and finally measure the time shift between multiple reflections of the stress pulse in the bar. This method however faces some major difficulties:

- because of the –non zero– rise time of the pulse, it is not perfectly square and precisely identifying a specific point on the pulse is difficult. Possibly noisy measurement can make this task even harder;
- the propagation in bars of finite diameter is dispersive [4] and so the shape of the pulse travelling down the bar is affected. It is also hard to find the time shift between two pulses with slightly different shape.

That is why in this article we introduce a method from precisely determining the velocity c_0, still from an impact test, but using the impact spectrum rather than the impact time series. Indeed, there is a link between the resonance frequencies –which appear in the impact spectrum– and the velocity of the bar c_0.

This article is organised as follows. The first part (Section 2) recalls the computation of the longitudinal resonance frequencies of a finite length rod. In Section 3, we derive the expression of the velocity as function of resonance frequencies and also compute the associated uncertainty. Finally, in Section 4 we show the efficiency of the proposed method on a concrete example.

2 Longitudinal modes of a finite length rod

Let L be the length of the bar, d the diameter of the bar. Let E, ρ and ν be respectively the modulus of elasticity, the density and the Poisson's ratio of the bar. In the following, the strain gauge is supposed to be positioned right in the middle of the bar. This should not theoretically be a restriction of the proposed method, only the antiresonances would differ. However, our strain gauges were glued in the middle of the bars in order to minimize pulse overlay between the incident and reflected waves.

2.1 1D solution

The wave equation of longitudinal waves in thin rods is [5] (pp77, (2.1.7)))

$$\frac{\partial^2 u}{\partial t^2} + \frac{E}{\rho}\frac{\partial^2 u}{\partial x^2} = 0 \tag{3}$$

where $u(x,t)$ is the displacement at coordinate x and time t. We can define the velocity of the bar $c_0 = \sqrt{E/\rho}$.

Stationary solution $u(x,t) = U(t)\Phi(x)$ and

$$\ddot{U}\Phi + c_0^2 U\Phi" = 0 \tag{4}$$

where the dot denotes derivative with respect to the time variable t and the prime denotes the derivative with respect to the space variable x.

$$\frac{\ddot{U}}{U} = -c_0^2\frac{\Phi"}{\Phi} = -\omega^2, \qquad \forall x,\ \forall t \tag{5}$$

where ω is the circular frequency. The longitudinal modes are the solutions of

$$\Phi" - \frac{\omega^2}{c_0^2}\Phi = 0 \tag{6}$$

Let $\lambda^2 = \omega^2/c_0^2$. The solutions of Eq. 6 are of the form

$$\Phi(x) = A\sin(\lambda x) + B\cos(\lambda x) \tag{7}$$

$$\Phi'(x) = \lambda A\cos(\lambda x) - \lambda B\sin(\lambda x) \tag{8}$$

where the constants A and B are determined from the boundary conditions, which are a null strain at $x = 0$ and $x = L$

$$\Phi'(0) = \lambda A \tag{9}$$

$$\Phi'(L) = -\lambda B\sin(\lambda L) \tag{10}$$

A null strain at the ends of the rod implies $A = 0$ and if we seek a non trivial solution (ie. $B \neq 0$) Eq. 10 becomes $\sin(\lambda L) = 0$. The longitudinal modes of the rod must therefore satisfy

$$\lambda_n = \frac{n\pi}{L},\ n \in \mathbb{N} \tag{11}$$

The eigenfrequencies of the rod are

$$f_n = \frac{nc_0}{2L},\ n \in \mathbb{N} \tag{12}$$

2.2 Antiresonances

Since the strain gauges are placed right at the middle of the bars, we need to identify the modes that also correspond to antiresonances. The additional condition for a mode to also be an antiresonance is

$$\Phi'(L/2) = 0 \tag{13}$$

From Eq. 8 a non trivial solution still implies $\sin(\lambda L/2) = 0$. The antiresonances therefore verify

$$\lambda = \frac{2n\pi}{L},\ n \in \mathbb{N} \tag{14}$$

The corresponding frequencies of the antiresonances are

$$f_{2n} = \frac{(2n)c_0}{2L},\ n \in \mathbb{N} \tag{15}$$

2.3 Observable resonances

In the case of a strain gauge located right in the middle of the rod, from Eq. 12 and Eq. 15 we can deduce that the observable resonances of the rod are

$$f_{2n+1} = \frac{(2n+1)c_0}{2L},\ n \in \mathbb{N} \tag{16}$$

2.4 1D solution with Love correction for the dispersion effects

The effect of the lateral inertia of the bar can be taken into account in the wave equation of the bar (see [6]; or [5], page 120: Love's equation of motion (2.5.61)). This leads to the following dispersive wave equation

$$\frac{\partial^2 u}{\partial x^2} + \frac{\nu^2 \rho J}{EA} \frac{\partial^4 u}{\partial x^2 \partial t^2} = \frac{\rho}{E} \frac{\partial^2 u}{\partial t^2} \tag{17}$$

where A is the section of the rod and J the polar moment of inertia. Let $\alpha^2 = \frac{\nu^2 \rho J}{EA}$ and still $c_0^2 = \frac{E}{\rho}$. In the case of a circular cross section with diameter d, we have $\alpha^2 = \frac{\nu^2 d^2}{8 c_0^2}$. Looking for a stationary solution of the form $u(x,t) = U(t)\Phi(x)$, Eq. 17 becomes

$$U\Phi" + \alpha^2 \ddot{U}\Phi" = \frac{1}{c_0^2} \ddot{U}\Phi \tag{18}$$

It is rewritten as

$$\frac{\ddot{U}}{U} = \frac{\Phi"}{\Phi/c_0^2 - \alpha^2 \Phi"} = -\omega^2, \qquad \forall x,\ \forall t \tag{19}$$

Solving this equation the same way as in section 2.1, we get the following condition for the resonances

$$\lambda = \frac{\omega}{c_0 \sqrt{1 - \omega^2 \alpha^2}} = \frac{n\pi}{L},\ n \in \mathbb{N} \tag{20}$$

Again, if we keep only the observable resonances and substitute the expression of α^2 into Eq. 20, we can get the value of c_0

$$c_0 = f_{2n+1} \sqrt{\left(\frac{2L}{2n+1}\right)^2 + \frac{(\pi \nu d)^2}{2}},\ n \in \mathbb{N} \tag{21}$$

3 Compute c_0 velocity and associated uncertainty from impact test

3.1 Velocity from impact test spectrum

The main idea of this article is that by performing an impact test on a bar of the SHPB device it is possible to get the value of c_0 and the associated uncertainty.

3.1.1 1D rod theory for longitudinal modes

If we consider the observable resonances of Eq. 16, we can deduce the velocity c from the f_{2n+1} peaks in the spectrum of the impact response of the bar

$$c(f_{2n+1}) = \frac{2L f_{2n+1}}{2n+1},\ n \in \mathbb{N} \tag{22}$$

This is indeed a way to get the velocity of waves at discrete frequencies f_{2n+1}, and not c_0, since in reality the wave propagation in the bar is dispersive ([4], [7]): the different wavelengths do not travel down the bar at the same speed and the velocity is therefore frequency dependent.

3.1.2 1D rod theory with Love correction for longitudinal modes

When we take the radial inertia into account, and contrary to the post-treatment with Eq. 22, it is possible to deduce the value of c_0 from the observable resonance frequencies f_{2n+1}

$$c_0 = f_{2n+1}\sqrt{\left(\frac{2L}{2n+1}\right)^2 + \frac{(\pi\nu d)^2}{2}},\ n \in \mathbb{N} \tag{23}$$

Note that removing the correction term $\pi\nu d^2/2$ in the previous equation leads to Eq. 22 for the simple 1D theory.

Of course Eq. 23 is only acceptable in low frequency: as the frequency increases, the correction for radial inertia is no longer sufficient and the resulting dispersion curve moves away from the Pochhammer dispersion curve (see figure 4 of [6] for a comparison of Pochhammer and Love dispersion curves).

3.2 Uncertainty in the value of the velocity

In the following, we use the notations defined in the GUM (guide to the expression of measurement uncertainty [8]) and the VIM (international vocabulary of metrology [9]). Let $u(x_1)$ denote the standard –in the sense of standard deviation– measurement uncertainty in x_1, it will be abbreviated as "uncertainty in x_1". The standard relative measurement uncertainty in x_1 is therefore $u(x_1)/x_1$, it will be abbreviated as "relative uncertainty in x_1".

The general rule for computing the uncertainty in the output of a functional relationship $y = f(x_i)$, with the assumption of uncorrelated inputs, is given in [8] (section 5.1.2, equation 10)

$$u^2(y) = \sum_{i=1}^{N}\left(\frac{\partial f}{\partial x_i}\right)^2 u^2(x_i) \tag{24}$$

3.2.1 1D rod theory for longitudinal modes

Eq. 22 is a functional relationship between input quantities L and f_{2n+1} and the output quantity $c(f_{2n+1})$. In [10], the reader can find a set of rules (see table 2 in [10]) for the most common functional relationships; this set of rules is only the application of Eq. 24. In the case of a fractionnal relationship of the type

$$y = \frac{Ax_1}{Bx_2} \tag{25}$$

where A and B are constants with no uncertainty, the uncertainty in the output is

$$\left[\frac{u(y)}{y}\right]^2 = \left[\frac{u(x_1)}{x_1}\right]^2 + \left[\frac{u(x_2)}{x_2}\right]^2 \tag{26}$$

Applying the rule of Eq. 26 to Eq. 22 gives the relative uncertainty in the computed velocity

$$\left[\frac{u(c)}{c}\right]^2 = \left[\frac{u(L)}{L}\right]^2 + \left[\frac{u(f_{2n+1})}{f_{2n+1}}\right]^2 \tag{27}$$

3.2.2 1D rod theory with Love correction for longitudinal modes

The equation of the velocity with Love correction (Eq. 23) is slightly more complicated when it comes to evaluate the associated uncertainty. Using the set of rules defined in table 2 of [10] is not sufficient and it is necessary to also use the primary definition Eq. 24.

In the case of a power relationship of the type

$$y = x_1^A \tag{28}$$

where A is a constant with no uncertainty the uncertainty in the output y is

$$\frac{u(y)}{y} = |A| \frac{u(x_1)}{x_1} \tag{29}$$

Writing Eq. 23 as $c_0 = f\sqrt{(\Gamma)}$ and using the rules of Eq. 26 and Eq. 29 we get

$$\left[\frac{u\left(c_0\right)}{c_0}\right]^2 = \left[\frac{u\left(f_{2n+1}\right)}{f_{2n+1}}\right]^2 + \frac{1}{4}\left[\frac{u\left(\Gamma\right)}{\Gamma}\right]^2 \tag{30}$$

We then need the general definition Eq.24 to write

$$u^2(\Gamma) = \left(\frac{2L}{2n+1}\right)^4 4L^2u^2(L) + \left(\frac{\pi d}{2}\right)^4 4\nu^2u^2(\nu) + \left(\frac{\pi\nu}{2}\right)^4 4d^2u^2(d) \tag{31}$$

Finally, combining Eq. 31 and Eq. 30 gives

$$\left[\frac{u\left(c_0\right)}{c_0}\right]^2 = \left[\frac{u\left(f_{2n+1}\right)}{f_{2n+1}}\right]^2 + \frac{1}{\left[\left(\frac{2L}{2n+1}\right)^2 + \left(\frac{\pi\nu d}{2}\right)^2\right]^2}\left[\left(\frac{2}{2n+1}\right)^4 L^4\left[\frac{u\left(L\right)}{L}\right]^2 + \left(\frac{\pi d}{2}\right)^4 \nu^4\left[\frac{u\left(\nu\right)}{\nu}\right]^2 + \left(\frac{\pi\nu}{2}\right)^4 d^4\left[\frac{u\left(d\right)}{d}\right]^2\right] \tag{32}$$

4 Application to 17-4PH steel bars

4.1 Impact test conditions

The present method is applied on the specific SHPB device designed and built at our laboratory, LBMC UMR_T9406 (Iffstar/UCLB). The measuring bars are made of Armco 17-4PH precipitation-hardening steel.

The Poisson's ratio of 17-4PH steel is $\nu = 0.291$ according to the manufacturer. The uncertainty on ν concerns its last significant digit (0.29**1**) and following [11] (Rule 1, page 23), the absolute uncertainty on ν is taken as $u(\nu) = 0.0005$.

The diameter of the bars is $d = 31.75\,\text{mm}$, the bars were centerless ground to obtain a precise diameter, a good cylindricity and a low surface roughness. The diameter is measured at several points and ranges from $31.71\,\text{mm}$ to $31.76\,\text{mm}$, so the absolute uncertainty on the diameter is taken as $u(d) = 0.025\,\text{mm}$.

The end surfaces of the bars were machined on a lathe. The length of the bars is $3058\,\text{mm}$, it is measured with a class II measuring tape. Directive 2014/32/EU [12] (Annex X, Chapter 1) gives the maximum permissible error (MPE) between two consecutive scale marks as $a + bL_r$, where $a = 0.3\,\text{mm}$, $b = 0.2$ and L_r is the value of the length rounded to the next whole metre ($L_r = 4\,\text{m}$ here).

The test for determining the value of c_0 is a single bar test: the strain wave is therefore reflected back and forth at the free ends of the bar. The steel impactor has a cylindrical shape; its diameter is $30.0\,\text{mm}$ and

Parameter x	unit -	value -	uncertainty $u(x)$	relative uncert. $u(x)/x$
L	m	3.058	0.0011	0.36×10^{-3}
d	mm	31.75	0.1	6.30×10^{-3}
ν	-	0.291	0.0005	1.72×10^{-3}
f_{2n+1}	Hz	-	5.23	-

Table 1: Summary of the SHPB setup characteristics

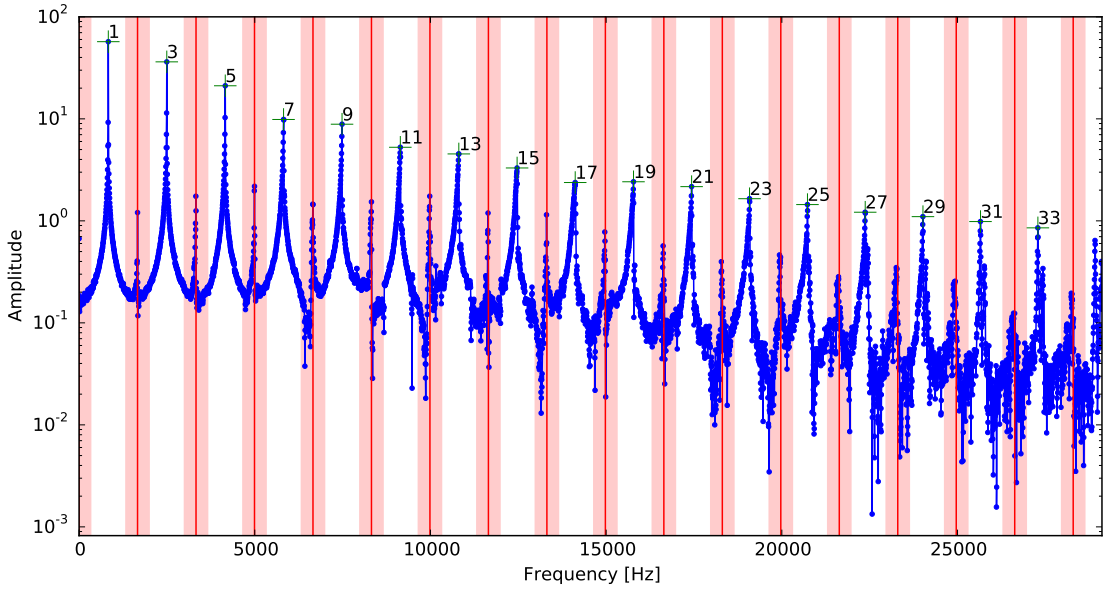

Figure 1: Frequency spectrum of the impact test (+: identified f_{2n+1} peaks with the corresponding value of $2n+1$; |: rough frequency f_{2n} of antiresonances; : discarded peak search zone)

its length is 94.2 mm. Using a short impactor is a way to have a high frequency content in the strain wave generated by the impact. The speed of the impactor just before impact is $23\,\mathrm{m\,s^{-1}}$; this parameter is indeed not important for the determination of c_0 as changing the striker velocity does not change the duration of the pulse.

The useful part of the signal is the part which contains the multiple reflections of the pulse in the bar. Its duration is 191 ms and during the time interval the pulse travels approximately 160 times the length $2L$.

Table 1 summarizes all the parameters values and uncertainties.

4.2 Peaks detection in frequency spectrum

Figure 1 illustrates the frequency spectrum of the impact test. The resonances are clearly visible. The peaks are automatically detected as the points with maximum amplitude between two antiresonances. The antiresonances are roughly determined using a first estimate of the velocity c_0 and Eq. 15. Because the spectrum becomes noisy as the frequency increases, especially around antiresonances, the peak search zone is reduced to 60 % of the frequency interval between two successive antiresonances by avoiding the light red bands (see Figure 1).

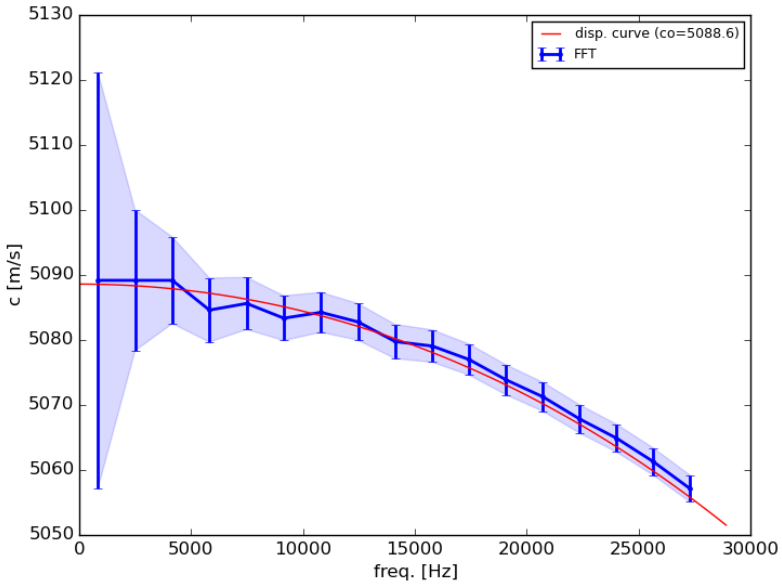

Figure 2: Velocity of the longitudinal waves and associated uncertainty with respect to frequency. The red curve is the exact dispersion curve computed with $c_0 = 5088.6\,\mathrm{m\,s^{-1}}$.

4.3 Velocity with 1D approach

Figure 2 illustrates the posttreatment of the impact spectrum with the 1D approach (see Eq.22). We also computed the numerical solution to the Pochhammer equation (red curve on Figure 2, see [13] for details on the computation) and it stays inside the corridor defined by the measurement uncertainty. This shows that we indeed computed $c(f_{2n+1})$ –and not c_0– as it is very close to the dispersion curve.

The uncertainty on the velocity decreases as the frequency increases (see Figure 3). This is due to the frequency term in Eq. 27: $u(f_{2n+1})$ is constant and taken equal to the frequency resolution in the frequency domain; it is inversely proportional to the duration of the time window of the impact signal. On the contrary, $\left[\frac{u(L)}{L}\right]^2$ is constant whatever the considered peak. From Eq. 27 it is clear that the uncertainty in c tends asymptotically to the value of the uncertainty in L as the frequency increases.

4.4 Velocity with Love correction approach

Figure 4 illustrates the posttreatment of the impact spectrum with the 1D approach with Love correction (see Eq.23). The Love correction removes the dispersive effect due to the finite diameter of the bar [5], that is why we can directly obtain the velocity c_0 from this graph.

Considering the uncertainty corridor, the points in Figure 4 are remarkably well aligned. That is why the velocity c_0 is computed by averaging the celerities $c_0^{(2n+1)}$ weighted by their respective inverse uncertainties (ie. $1/u(c_0^{(2n+1)})$). From the impact test posttreated with Love correction, the average velocity is $5088.63\,\mathrm{m\,s^{-1}}$. The uncertainty on the last point (highest frequency) is $u(c_0) = 2.07\,\mathrm{m\,s^{-1}}$. The relative uncertainty is $u(c_0)/c_0 = 0.41 \times 10^{-3}$, which is very close to the relative uncertainty in the length of the bar (which can also be observed in Figure 3).

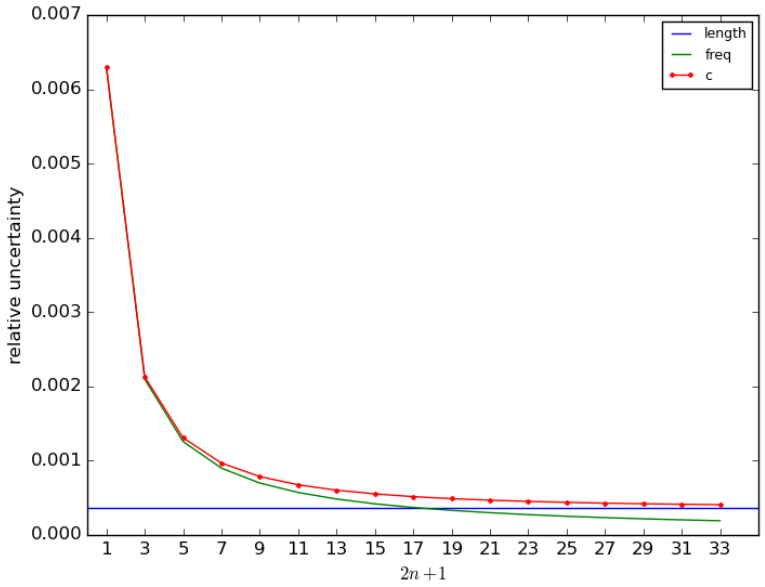

Figure 3: Values of the relative uncertainty in the velocity $u(c)/c$, in the frequency $u(f_{2n+1})/f_{2n+1}$ and in the length $u(L)/L$ with respect to the frequency index $2n + 1$

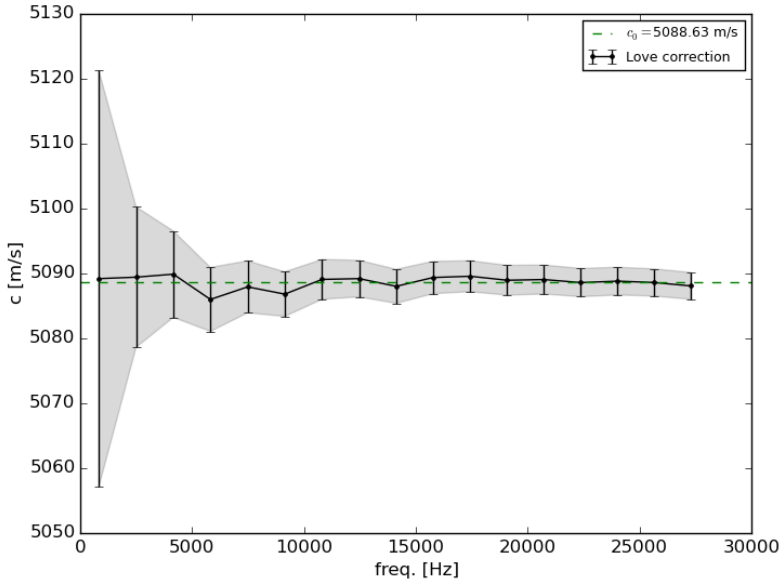

Figure 4: Velocity c_0 and associated uncertainty. Posttreatment of the impact test with Love correction.

5 Conclusion

We introduced a method for the precise determination of the velocity c_0 of SHPB measurement bars. This method is based on a simple impact test on a single bar, which is –of course– an easy experiment to perform on SHPB device. By working on the spectrum of this impact test, it is possible to easily identify sharp peaks that correspond to the resonance frequencies of the bar. The longitudinal modes of the bar give the relationship between the frequency of these peaks and the velocity c_0. We also expressed the uncertainty in the measurement of c_0 and showed in our case the relative uncertainty in c_0 is close to the uncertainty in the length of the bar, ie. around $0.04\,\%$. In the context of quality in measurement with SHPB, this is an important first step which then enables to assess the uncertainty in the strain and strain rate in the sample.

References

[1] Howard Kuhn. *ASM Handbook: Volume 8: Mechanical Testing and Evaluation*, volume 8. ASM International, 10 edition, September 2000.

[2] Bazle A Gama, Sergey L Lopatnikov, and John W Gillespie. Hopkinson bar experimental technique: A critical review. *Applied Mechanics Reviews*, 57(4):223, 2004.

[3] Zhouhua Li and John Lambros. Determination of the dynamic response of brittle composites by the use of the split Hopkinson pressure bar. *Composites Science and Technology*, 59(7):1097–1107, May 1999.

[4] Dennison Bancroft. The Velocity of Longitudinal Waves in Cylindrical Bars. *Physical Review*, 59(7):588–593, 1941.

[5] Karl F. Graff. *Wave Motion in Elastic Solids*. Dover Publications, June 1991.

[6] Simon P. Anderson. Higher-order rod approximations for the propagation of longitudinal stress waves in elastic bars. *Journal of Sound and Vibration*, 290(1):290–308, February 2006.

[7] R. M. Davies. A Critical Study of the Hopkinson Pressure Bar. *Philosophical Transactions of the Royal Society of London A: Mathematical, Physical and Engineering Sciences*, 240(821):375–457, January 1948.

[8] Evaluation of measurement data – Guide to the expression of uncertainty in measurement. JCGM 100: 2008 (GUM 1995 with minor corrections), BIPM Joint Committee for Guides in Metrology, Paris, 2008.

[9] International vocabulary of metrology – Basic and general concepts and associated terms, 3rd edn. JCGM 200: 2008 (VIM), BIPM Joint Committee for Guides in Metrology, Paris, 2008.

[10] Ian Farrance and Robert Frenkel. Uncertainty of Measurement: A Review of the Rules for Calculating Uncertainty Components through Functional Relationships. *The Clinical Biochemist Reviews*, 33(2):49–75, May 2012.

[11] Les Kirkup and Bob Frenkel. *An Introduction to Uncertainty in Measurement: Using the GUM (Guide to the Expression of Uncertainty in Measurement)*. Cambridge Universtity Press, Cambridge, 2006.

[12] Directive 2014/32/EU of the European Parliament and of the Council of 26 February 2014 on the harmonisation of the laws of the Member States relating to the making available on the market of measuring instruments (recast), February 2014.

[13] D. Brizard, S. Ronel, and E. Jacquelin. Estimating Measurement Uncertainty on Stress-Strain Curves from SHPB. *Experimental Mechanics*, 57(5):735–742, June 2017.